

BRIEF COMMUNICATION

A TRANSIENT UNIDIMENSIONAL TWO-PHASE FLOW MODEL AND ITS APPLICATION TO A SPARK IGNITION ENGINE

S. C. Low

School of Mechanical & Production Engineering, Nanyang Technological Institute, Singapore 2263

(Received 25 November 1986; in revised form 20 November 1987)

1. INTRODUCTION

The lean burn spark ignition engine is reckoned to be an attractive proposition in engine design because it meets the legislative emission requirements and offers better fuel economy. However, Germane *et al.* (1983) indicated that the performance of the lean burn engine was critically dependent on the air-fuel mixture distribution to the cylinders. The variation of mixture strength could lead to a severe surge in output torque due to the mixture strength variation. In order to understand the transportation and distribution of the air-fuel mixture, Liu *et al.* (1984) studied the evaporation of fuel droplets during the suction process. The transient fuel flow pattern has been investigated by Fujieda & Ohya (1985) and Hohsho *et al.* (1985) Yun *et al.* (1976), Lo & Lalas (1977), Lo (1976) and Boam & Finlay (1979) undertook studies on the one-dimensional steady flow of droplets and air in an idealized manifold system based on the model of Habib (1975). Low & Baruah (1981) used a characteristics method to solve the two-phase flow problem in a straight pipe, however, the application was confined to steady flow. As the air flow in the engine intake system is highly pulsatory and the fuel supplied is time-varying, a non-steady fuel droplet and air flow model is therefore developed to enable the study of the fuel droplet behaviour in the pulsatory air flow process.

2. THEORETICAL CONSIDERATION

Assumptions

- (a) Lean fuel-air ratio (about 1:15 by wt and about 1:10,000 by vol), hence the volume of liquid fuel is neglected.
- (b) Spherical droplets.
- (c) No chemical reaction, droplet shattering or droplet coalescence.
- (d) No temperature gradient within the droplet since the radius is $< 50 \mu\text{m}$.
- (e) Droplets are evenly distributed over the cross-section of the pipe.
- (f) The turbulent air motion is not included, however, its effects on heat, mass and momentum transfer are taken into consideration when choosing the empirical equations.
- (g) Separate sets of equations are developed for the gaseous and liquid phases. The two phases are then coupled through the exchanges of heat, momentum and mass.

Gaseous phase

The one-dimensional continuity, momentum and energy equations of the gaseous phase with liquid fuel evaporation can be expressed as

$$\frac{\partial \rho}{\partial t} + \frac{1}{A_c} \frac{\partial}{\partial x} (\rho u A_c) = \Gamma_d^m, \quad [1]$$

$$\frac{\partial}{\partial t}(\rho u) + \frac{1}{A_c} \frac{\partial}{\partial x}(\rho u^2 A_c) + \frac{\partial P}{\partial x} = \Gamma_d^m(u - v) + \Gamma_d^f + \Gamma_w^f \quad [2]$$

and

$$\frac{\partial}{\partial t} \left[\rho \left(h - RT + \frac{u^2}{2} \right) \right] + \frac{1}{A_c} \frac{\partial}{\partial x} \left[\rho u A_c \left(h + \frac{u^2}{2} \right) \right] - \Gamma_d^m h_{dG}^\circ = \Gamma_d^e + \Gamma_w^e, \quad [3]$$

where t , x , u , ρ , T , h , P , A_c and v are the time, distance, gas velocity, density, temperature, enthalpy, pressure, pipe cross-sectional area and the droplet velocity, respectively; Γ is the transport property per unit volume; the superscripts e, f and m designate heat transfer, momentum transfer and mass transfer, respectively; the subscript d designates the droplet phase and w designates the pipe wall; h_{dG}° is the stagnation enthalpy of the evaporated fuel.

Manipulation of [1]–[3] gives

$$\left[\frac{\partial P}{\partial t} + (u + a) \frac{\partial P}{\partial x} \right] + \rho a \left[\frac{\partial u}{\partial t} + (u + a) \frac{\partial u}{\partial x} \right] + \tau_1 + \tau_2 + \tau_3 = 0, \quad [4]$$

$$\left[\frac{\partial P}{\partial t} + (u - a) \frac{\partial P}{\partial x} \right] + \rho a \left[\frac{\partial u}{\partial t} + (u - a) \frac{\partial u}{\partial x} \right] + \tau_1 + \tau_2 - \tau_3 = 0 \quad [5]$$

and

$$\left(\frac{\partial P}{\partial t} + u \frac{\partial P}{\partial x} \right) - a^2 \left(\frac{\partial \rho}{\partial t} + u \frac{\partial \rho}{\partial x} \right) + \tau_1 = 0, \quad [6]$$

where

$$\tau_1 = -(\gamma - 1) \left\{ \Gamma_w^e + u \Gamma_w^f + \left[-\Gamma_d^e + \Gamma_d^f(u - v) - \Gamma_d^m(h_G^\circ - h_{dG}^\circ - u^2 + uv) \right] \right\} \quad [7]$$

$$\tau_2 = \frac{\rho a^2 u}{A_c} \frac{dA_c}{dx} - a^2 \Gamma_d^m \quad [8]$$

and

$$\tau_3 = a \Gamma_w^f + a \left(u \Gamma_d^m - v \Gamma_d^m + \Gamma_d^f \right); \quad [9]$$

h_G° is the stagnation enthalpy of gas, a is the speed of sound and γ is the isentropic index.

By adopting the work of Benson *et al.* (1964), whose λ and β characteristics are defined as

$$\lambda = A + \frac{\gamma - 1}{2} U \quad \text{along the path} \quad \left[\frac{dx}{dt} \right]_\lambda = u + a$$

and

$$\beta = A - \frac{\gamma - 1}{2} U \quad \text{along the path} \quad \left[\frac{dx}{dt} \right]_\beta = u - a,$$

where A and U are the non-dimensional speed of sound and gas velocity, respectively; the change in the Riemann variables (λ and β) along the characteristics can be written as

$$d\lambda = -\frac{\gamma - 1}{2\rho A a_{ref}^2} (\tau_1 + \tau_2 + \tau_3) dt + A \frac{dA_A}{A_A} \quad [10]$$

and

$$d\beta = -\frac{\gamma - 1}{2\rho A a_{ref}^2} (\tau_1 + \tau_2 - \tau_3) dt + A \frac{dA_A}{A_A} \quad [11]$$

where the subscript ref represents the reference condition. The gas particle “path line” is defined as

$$\left[\frac{dx}{dt} \right]_G = u$$

along which the change in “entropy” is

$$dA_A = -A_A \frac{\tau_1}{2\rho A^2 a_{ref}^2} dt. \tag{12}$$

Liquid (fuel droplets) phase

The direction of the droplet “path line” is

$$\left[\frac{dx}{dt} \right]_d = v_i,$$

where v_i is the droplet velocity. The change in droplet properties (radius r_i , temperature T_i and velocity v_i) along the path line can be related by

$$\frac{dr_i}{dt} = \frac{W_i}{4\pi r_i^2 \rho_d}, \tag{13}$$

$$\frac{dT_i}{dt} = \frac{Q_i - W_i L}{\frac{4}{3}\pi r_i^3 \rho_d C_{pdf}} \tag{14}$$

and

$$\frac{dv_i}{dt} = \frac{F_i}{\frac{4}{3}\pi r_i^3 \rho_d}, \tag{15}$$

where ρ_d is the fuel density, L is the latent heat of evaporation and C_{pdf} is the specific heat of the fuel droplet.

The rate of evaporation W_i , rate of heat transfer Q_i and drag F_i on the droplet i can be determined by the interactions between the droplet and the gaseous phase.

Interaction between the gaseous and liquid phases

Liquid phase. When a droplet i is entrained in a gaseous phase of known velocity (u), temperature (T) and pressure (P), the mass and heat transfer can be calculated by the equations suggested by Priem & Heidmann (1960):

$$W_i = 4\pi r_i^2 K P_v \frac{P}{P_v} \ln \left[\frac{P}{(P - P_v)} \right], \tag{16}$$

where K is the mass transfer coefficient and P_v is the fuel vapour pressure; and

$$Q_i = 4\pi r_i^2 h (T - T_i) \theta, \tag{17}$$

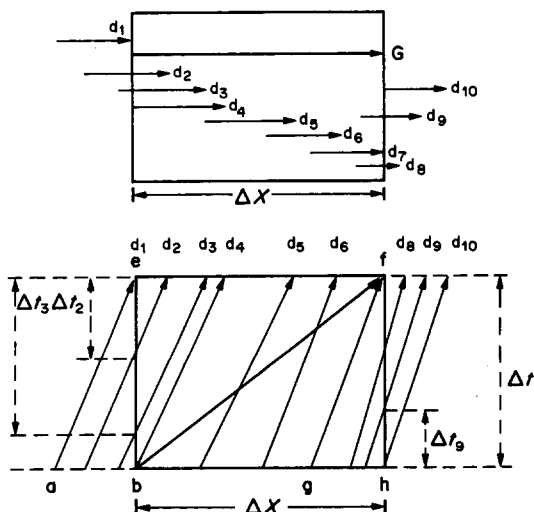


Figure 1. Interaction between the characteristic and the droplet path lines.

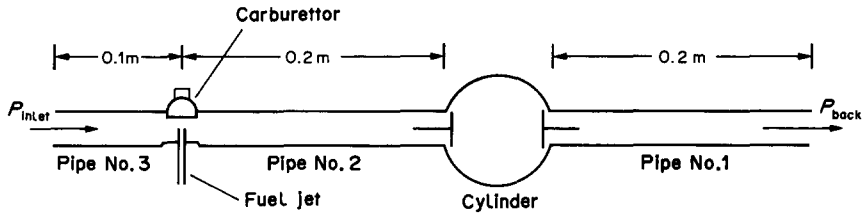


Figure 2. The inlet and exhaust system of a spark ignition engine.

where h is the heat transfer coefficient and θ is a correction factor proposed by Priem & Heidmann (1960).

For momentum transfer, the Ingebo (1956) drag model is adopted:

$$F_i = \frac{\frac{1}{2}\pi r_i^2 \rho (u - v_i) |u - v_i| 27}{Re_i^{0.84}}, \tag{18}$$

where Re_i is the Reynolds number of the droplet i .

With the known values of Q_i , W_i and F_i for a droplet path line the changes in T_i , r_i and v_i for the path line can be calculated using [13]–[15].

Gaseous phase. Figure 1 shows a control volume of length ΔX in which a characteristic, represented by the dark arrow, travels from one end of the control volume to the other within a step Δt . The rest of the arrows represent the loci of droplets. The residence time of droplet i within the control volume is Δt_i . Hence, the fraction of residence time of a droplet within the control volume can be expressed as $y_i = \Delta t_i / \Delta t$.

If there are N droplet path lines in a control volume, each representing n_i droplets per unit gas volume and having the fraction of resident time in the control volume y_i , by knowing the Q_i , W_i and F_i of all the path lines the heat, mass and momentum transfer in the control volume in duration Δt can be expressed as follows:

$$\Gamma_d^c = \sum_{i=1}^N n_i Q_i y_i, \quad \Gamma_d^m = \sum_{i=1}^N n_i W_i y_i \quad \text{and} \quad \Gamma_d^f = \sum_{i=1}^N n_i F_i y_i.$$

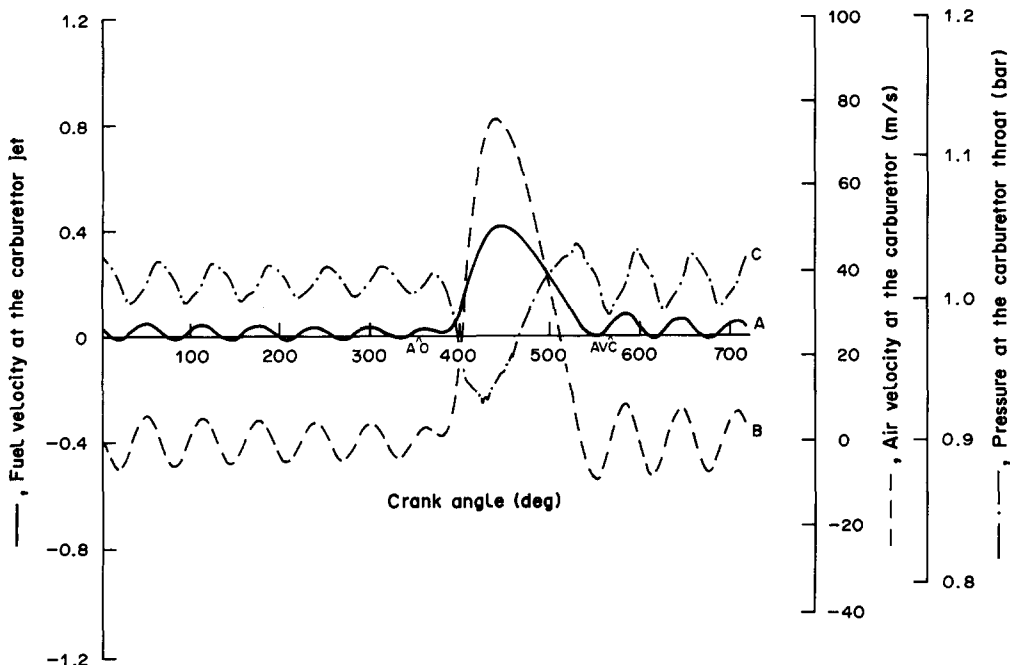


Figure 3. The instantaneous fuel velocity, air velocity and pressure at the carburettor; $R_d = 35 \mu\text{m}$.

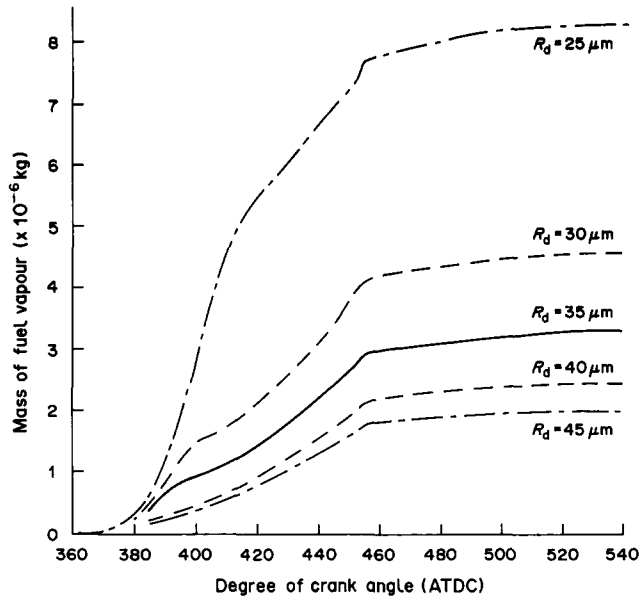


Figure 4. Cumulative fuel vapour charged into the cylinder.

With a known value of the characteristic (λ , β or A_A) at one end of the control volume, the change in the characteristic ($d\lambda$, $d\beta$ or dA_A) during its travel from one end of the control volume to the other can be calculated by [10]–[12] if the values of Γ_w^c , Γ_w^f , Γ_d^c , Γ_d^m , Γ_d^f , y_i and n_i are known.

If α is the mole ratio of fuel vapour to air registered on a gas path line at the entrance to a control volume, then the ratio at the exit should be:

$$\alpha' = \frac{\left(\alpha + \frac{1}{M_d} \Gamma_d^m \Delta t \right)}{\left(1 + \frac{1}{M_d} \Gamma_d^m \Delta t \right)}, \quad [19]$$

where M_d is the molecular weight of the fuel.

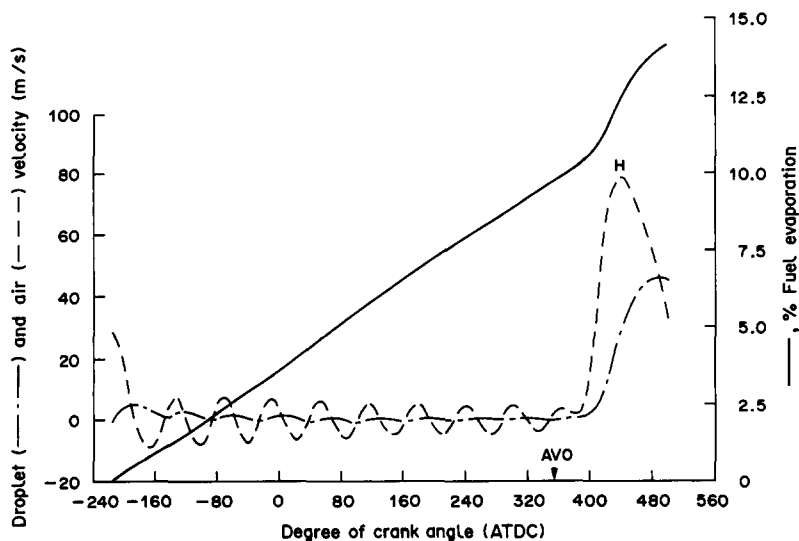


Figure 5. Evaporation and velocity of a droplet path line and the air velocity acting on it; $R_d = 35 \mu\text{m}$.

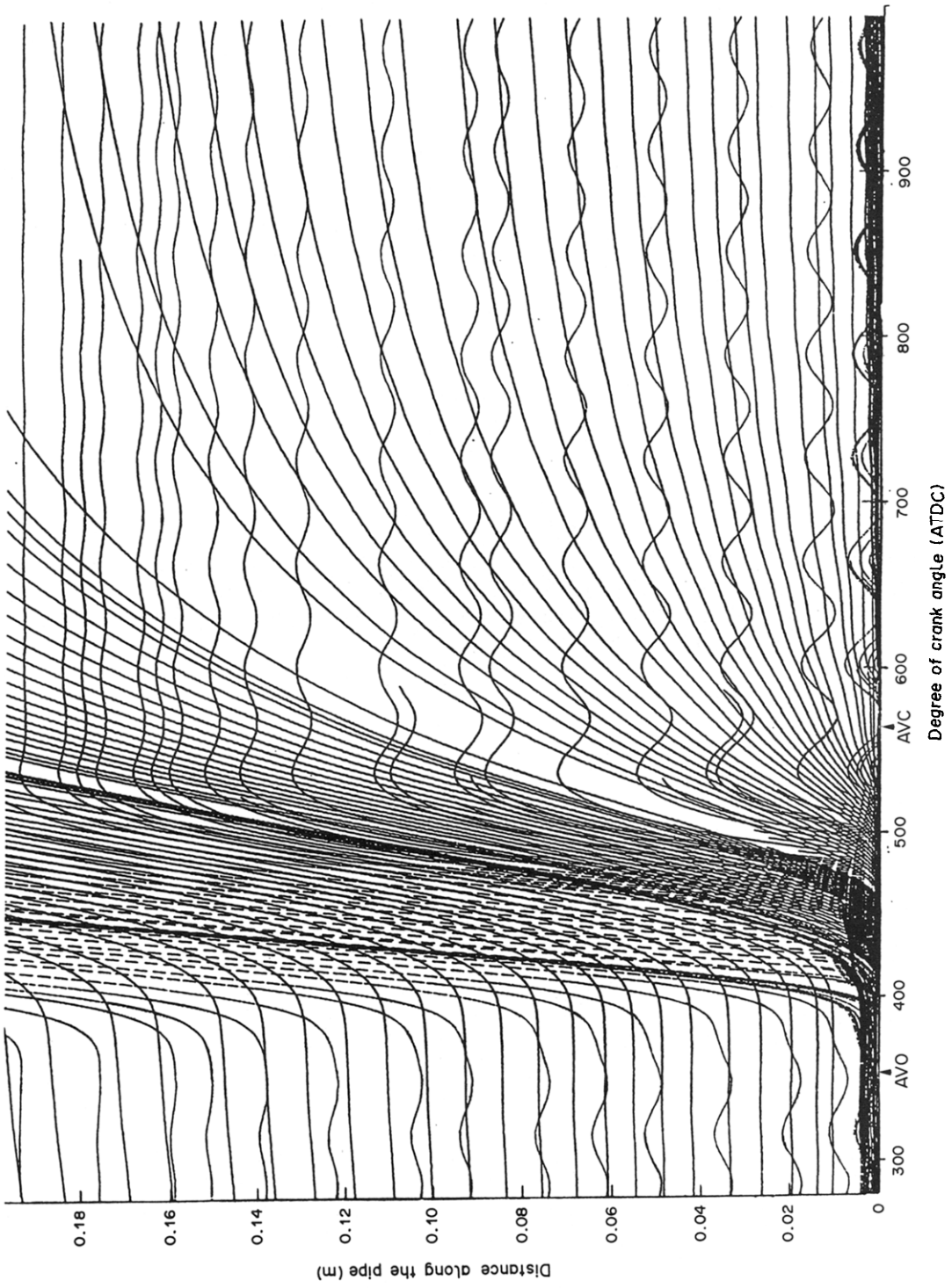


Figure 6. Loci of gas particle path lines (the relatively wavy curves) and droplet path lines for $R_0 = 45 \mu\text{m}$ (the relatively smooth curves) along pipe No. 2.

3. RESULTS AND DISCUSSION

The proposed characteristics scheme is solved by a method similar to that of Benson *et al.* (1964). It is applied to the solution of the equations describing the flow of fuel droplets and air in a single-cylinder four-stroke spark ignition engine, with both intake and exhaust systems, fitted with a constant depression carburettor. The simulated engine can be seen in figure 2. In this calculation, the engine speed was kept constant at 3000 rpm and the carburettor was at full throttle. There is a fuel jet tube at the carburettor bridge (throat), whose flow was calculated by a set of non-steady incompressible fuel flow equations developed by Low (1980).

Figure 3 shows the fluctuation of air velocity and pressure at the carburettor. In response to the pressure fluctuation, the carburettor jet delivered fuel into the air stream. It is observed that a small quantity of fuel is supplied from the jet while the engine inlet valve is closed.

A comparison of cumulative fuel vapour flow through the engine inlet valve within one engine cycle for droplets of differing initial sizes is shown in figure 4. Each curve can be sub-divided into two main portions. Initially, the engine sucks in the gas which resides in the inlet pipe following the closure of the engine inlet valve in the previous cycle. The relatively long residence time of the gas with the droplets results in a high fuel vapour air ratio in the gas. The entry of this portion of gas into the cylinder explains the initial rapid rise in cumulative vapour entering the cylinder. In the latter stage, pure air is sucked into the pipe, flows through the fuel droplets and eventually enters the cylinder. The amount of fuel vapour it could pick up is expected to be lower, simply due to the shorter residence time it has with the droplets before flowing into the cylinder.

Figure 5 shows the variation in properties for a typical droplet path line. The oscillatory air velocity has little effect on the droplet velocity before AVO, due to the high droplet inertia drag ratio. It is noted that during the suction period, the rate of fuel evaporation is greatly increased.

A complete picture of the loci of gas and droplet path lines used in the calculation for one complete engine cycle is shown in figure 6.

REFERENCES

- BENSON, R. S., GARG, R. D. & WOOLATT, D. 1964 A numerical solution of unsteady flow problems. *Int. J. mech. Sci.* **6**, 117–144.
- BOAM, D. J. & FINLAY, I. C. 1979 A computer model of fuel evaporation in the intake system of a carburetted petrol engine. In *Proc. IMechE. Conf. on the Fuel Economy and Emissions of Lean Burn Engines*, Paper C89/79, pp. 25–37.
- FUJIEDA, M. & OHYAMA, Y. 1985 Analysis of mixture transport delay in fuel supply for a carburetted engine. *Bull. JSME* **28**, 2034–2040.
- GERMANE, G. J., HESS, C. C. & WOOD, C. G. 1983 Lean combustion in spark-ignited internal combustion engines. SAE Paper No. 831217.
- HABIB, I. S. 1975 The interaction of a hot gas flow and a cold liquid spray. ASME Paper n75-HT-37.
- HOHSHO, Y., KANNO, K., NAKAI, H. & KADOTA, T. 1985 Characteristics of response of carburetted SI engine under transient condition. *Bull. JSME* **28**, 1725–1732.
- INGEBO, R. D. 1956 Drag coefficient for droplet and solid spheres in clouds accelerating in air streams. Report NACA TN 3762.
- LIU, X. Q., WANG, C. H. & LAW, C. K. 1984 Simulation of fuel droplet gasification in SI engine. *ASME JI Engng Gas Turbines Power Trans.* **106**, 849–853.
- LO, R. S. 1976 Investigation of fuel droplet flow in an idealized automotive engine induction system. Ph.D. Dissertation, Wayne State Univ., Detroit, Mich.
- LO, R. S. & LALAS, D. P. 1977 Parametric study of fuel droplet flow in an idealized engine induction system. SAE Paper No. 770645.
- LOW, S. C. 1980 Non-steady fuel-droplet and air flow in the intake manifold of a spark-ignition engine. Ph.D. Thesis, UMIST, Lancs., U.K.
- LOW, S. C. & BARUAH, P. C. 1981 Liquid fuel droplets entrained in the transient unidimensional gas flow in a pipe. *Int. J. Multiphase Flow* **7**, 293–309.

- PRIEM, R. J. & HEIDMANN, M. F. 1960 Propellant vaporization as a design criterion for rocket-engine combustion chambers. Report NASA TR R-67.
- YUN, H. J., LO, R. S. & NA, T. Y. 1976 Theoretical studies of fuel droplet evaporation and transportation in a carburettor venturi. SAE Paper No. 760289.